Modular synthesis of planar-chiral cycloalkenes via *trans*-retentive trapping of π-allyl-Pd dipoles

Zheng-Xin Zhou[1], Yue-Liu-Ting Fu[1], Yuan-Heng Li[2], Bin-Jun Zhang[1], Yu-Qing Xiao[1], Yu-Jie Li[1], Li-Yan Chen[1], Li Rao[1,*], Ying Tan[2,*], Liang-Qiu Lu[1,3,4,*] and Wen-Jing Xiao[1,5]

[1]Engineering Research Center of Photoenergy Utilization for Pollution Control and Carbon Reduction, Ministry of Education, College of Chemistry, Central China Normal University, 152 Luoyu Road, Wuhan 430079, China

[2]State Key Laboratory of Chemical Oncogenomics, Key Laboratory of Chemical Biology, Tsinghua Shenzhen International Graduate School, Tsinghua University, Shenzhen 518055, China

[5]State Key Laboratory for Oxo Synthesis and Selective Oxidation, Lanzhou Institute of Chemical Physics (LICP), Chinese Academy of Sciences, Lanzhou 730000, China

[4]School of Chemistry and Chemical Engineering, Henan Normal University, Xinxiang 453007, China

[5]Wuhan Institute of Photochemistry and Technology, Wuhan 430082, China

*Email: raoli@ccnu.edu.cn; tan.ying@sz.tsinghua.edu.cn; luliangqiu@ccnu.edu.cn

Abstract: Planar-chiral cycloalkenes are challenging synthetic targets due to the medium-sized ring and the *trans*-configured olefin. Asymmetric resolution of racemic *E*-cycloalkenes, UV-induced asymmetric isomerization of *Z*-cycloalkenes, and asymmetric intramolecular cyclization of olefinic substrates are known as the limited approaches to these scaffolds. However, these methods usually suffer from tedious synthesis, harsh conditions, and insufficient structural diversity. Here, we present a novel palladium-catalyzed asymmetric [7+2] cycloaddition to facilitate the modular synthesis of planar-chiral 9-membered cycloalkenes from readily available chemicals. Excellent selectivity for planar chirality was achieved by retaining the *trans*-2H configuration of the π-allyl-Pd species throughout the whole process. Mechanistic studies were performed to elucidate the pivotal role of hydrogen bonding from the chiral ligand in enhancing both reaction efficiency and stereocontrol. In addition, synthetic transformations of planar chiral cycloalkene products and their applications in the identification of anticancer agents and selective bioimaging of cancer cells demonstrated the synthetic value of this new methodology. This research provides a promising way to access synthetically valued planar-chiral cycloalkenes.

One-Sentence Summary: A modular platform for synthesizing planar-chiral cycloalkenes via *trans*-retentive trapping of π-allyl-Pd dipoles with ketenes is reported.

Planar chirality, caused by breaking the symmetry of a plane, is an important member of molecular chirality and has attracted increasing interest from the synthetic community, medicinal chemists, and materials scientists (Fig. 1A, *1-6*). Compared with central chirality (*7*) and axial chirality (*8*), planar chirality is still underdeveloped and in particular, the asymmetric catalytic synthesis of planar-chiral cycles is much less studied (*1*, *9-14*) than metallocenes (*15-17*). Recently, Collins et al. (*18*) reported a biocatalytic synthesis of planar-chiral macrolactones from benzylic-substituted diols and diacids (Fig. 1B, left). Almost simultaneously, Morinaka et al. (*19*) reported an enzymatic crosslinking of a tryptophan-containing linear peptide to form an indole-bridged planar-chiral cyclophane (Fig. 1B, right). In comparison, rigid cycloalkenes bearing medium-sized rings and *trans*-configured olefins are more unreachable owing to unfavorable entropic factors (*20*), challenging planar chirality, and stereochemical lability (*1*). Limited methods to approach these scaffolds include the asymmetric resolution of *E*-cycloalkenes (*21*), UV-induced asymmetric isomerization of *Z*-cycloalkenes (*22*), and intramolecular asymmetric cyclization of elaborate olefinic substrates (Fig. 1C, *9*, *23*). However, an efficient modular platform for the synthesis of significant planar-chiral cycloalkenes (*24*, *25*) from readily available starting materials is still largely unfulfilled.

Palladium-catalyzed cycloadditions involving π-allyl-Pd dipolar intermediates (ab. dipoles) have been identified as a powerful tool for the synthesis of cyclic molecules (*26*, *27*). In particular, owing to Zhao's important finding in 2017 (*28*) that the regioselectivity of Pd-catalyzed intramolecular allylic substitution can be switched from the usual branched selectivity (*29*, *30*) to linear selectivity, a number of medium-sized *cis*-cycloalkenes have been successfully prepared via *cis*-π-allyl-Pd dipoles (Fig. 1D, top, left, *31-36*). Following our research interest on heterocycle synthesis (*33*, *35*, *37-40*), we recently wondered whether asymmetric Pd-catalyzed cycloaddition via *trans*-π-allyl-Pd dipoles could be realized while retaining the linear selectivity and the *trans*-2H-configulation of π-allyl-metal (Fig. 1D, top, right,*41*). Thus, we were able to obtain planar-chiral cycloalkenes with high efficiency and selectivity. As shown in Fig. 1D (bottom), we proposed an asymmetric [7+2] cycloadditions between oxindole-derived vinyl cyclopropanes (ab. VCPs) and diazo reagents under the sequential Rh and Pd catalysis. This research documents our efforts on this topic, not only producing a variety of structural diverse indole-fused cycloalkenes with excellent enantio- and diastereoselectivities, but also disclosing unprecedented reaction mode of reactive π-allyl-Pd dipolar species.

Design plan

A detailed design plan for the Pd-catalyzed [7+2] cycloaddition is depicted in Fig. 2A. First, the oxidative addition of oxindole-derived VCPs **1** to Pd(0) was conducted to form *π*-allyl-Pd dipole **I** with a 2H-*trans*-configuration. This process was supported by the recently reported Pd-catalyzed [3+2] cycloadditions of VCPs **1** with Michael acceptors (*42*). However, unlike these known cycloadditions, the key *O*-addition of the enol unit to ketene **II**, generated in situ from diazoacetate reagents **2** by Rh-catalyzed Wolff rearrangement (*43*), was unknown and assumed here based on our recent research (*44*). Next, the corresponding adduct **III** was subjected to intramolecular allylic substitution to produce the desired 9-membered cycloalkenes **3**, leaving the *trans*-olefinic configuration. To achieve this goal, we need to overcome three potential challenges on selectivity control: 1) the chemoselectivity resulting from the competitive *C*-atom addition to the ketene (*40*) and eventually affording byproduct **A**; 2) the periselectivity associated with Pd-catalyzed allylic substitutions (linear selectivity to yield the desired product **3** or branched selectivity to yield the byproduct **B**); and 3) the stereoselectivity on the control of planar chirality, as well as chiral quaternary stereocenters (*45*, *46*).

Condition optimization

To examine the feasibility of the designed [7+2] cycloaddition, an initial study was performed using oxindole-derived VCP **1a'** and diazoacetate **2a'** as model substrates, $Rh_2(OAc)_4$ as the catalyst for ketene formation, and a combination of $Pd_2(dba)_3{\cdot}CHCl_3$ and chiral bisphosphine ligand **L1** as the catalyst for cycloaddition (Fig. 2B). In a one-pot stepwise operation, a solution of highly reactive ketene intermediates was prepared in situ from substrate **2a'**, which was then exposed to a solution of the Pd catalyst and substrate **1a'** in CH_2Cl_2. To our delight, the desired medium-sized cycloalkene **3a'** was obtained in 18% yield and with 43% ee and 2:1 dr after another 24 h without the formation of byproducts **A** and **B** (Fig. 2B, entry 1). Encouraged by this promising result, we investigated other chiral phosphine ligands in order to improve the reaction outcome. The enantioselectivity was significantly improved with biphosphine ligand **L3**, which was attributed to hydrogen-bonding interactions (entry 3: 17% yield, 86% ee, and 4:1 dr). However, the use of similar chiral ligand **L4** did not result in any conversion of starting material **1a'** (entry 4). In addition, variation in the reaction medium did not improve the enantioselectivity (entries 5–7). Replacing the methyl group of the VCP substrate (**1a'**) with a Boc group (**1a**) improved the reaction efficiency because of the higher reactivity of the latter, albeit with a slight loss of stereoselectivity (entry 8: 50% yield, 80% ee, and 3:1 dr). The absolute configurations of these two stereoisomers, **3a''** and **3a1''**, were determined by X-ray diffraction of the corresponding single crystals. Performing the reaction at low temperatures can improve the enantio- and diastereoselectivities (entries 9 and 10). The use of chiral biphosphine ligand **L5** (entry 11) and benzyl ester-substituted diazoacetate **2a** (entry 12) further improved the results. Finally, the optimal reaction conditions were identified (entry 12) and chiral product **3a** was obtained in 75% isolated yield with >99% ee and >19:1 dr.

Substrate scope

Next, we began to explore the scope of this asymmetric [7+2] cycloaddition. In general, a variety of VCPs and alkenyl-substituted diazoacetates were well suited for this transformation (Fig. 3). Variations in the electronic properties and substitution mode of the indole ring of the VCP substrates were tolerable, and the corresponding products were generally obtained in good yields with high enantio- and diastereoselectivities (Fig. 3, **3a**-**3f**: 51-76% yields, up to >99% ee and >19:1 dr). The replacement of the protecting group Boc with Cbz, Bz and Me, or avoidance of the protecting group were proved feasible, affording the desired products with good stereocontrol (**3g**-**3j**: 58-78% yields, up to 96% ee, and >19:1 dr). In addition, other alkenyl-substituted diazoacetates were investigated under the optimal reaction conditions. Variations in the ester moiety (Et, *i*-Pr, and *t*-Bu) or the use of 1-propenyl and (thiophen-2-yl)vinyl moiety were found to be compatible and afforded structurally diverse cycloalkene products **3k**-**3m** in 68-74% yields with high enantioselectivities ranging from 87% to >99% ee and excellent diastereoselectivities. In addition to alkenyl-substituted diazoacetates, aryl-substituted diazoacetates have been used in asymmetric cycloadditions. A series of VCPs reacted with phenyl-substituted methyl diazoacetate **4a**, affording structurally varied cycloalkenes in moderate to good yields with generally excellent enantio- and diastereoselectivities (**5a**-**5f:** 44-84% yields, 90-96% ee and >19:1 dr). Subsequently, we investigated various aryl-substituted diazoacetate substrates and found that in addition to methyl esters, *n*-butyl and *t*-butyl esters can also be applied to this catalytic system, affording the corresponding planar-chiral cycloalkenes **5g** and **5h** with excellent enantio- and diastereoselectivities. Moreover, diazoacetates with electron-rich and electron-deficient phenyls, heteroaryls, and even ferrocenyl groups were found to be successful in this cycloaddition, producing the corresponding products **5i**–**5s** in moderate to good yields with

excellent enantio- and diastereoselectivities (45-85% yields, up to >99% ee and >19:1 dr). Furthermore, a biester-substituted diazo compound was also examined by switching the Rh-catalyzed Wolff rearrangement to a photo-Wolff rearrangement. Promisingly, product **5t** with a single planar chirality was successfully obtained in 38% yield and 73% ee.

Mechanistic investigations

To better understand the origin of this stereochemistry, both experimental and computational studies of the Pd-catalyzed asymmetric [7+2] reaction were conducted. First, a control experiment was performed using *N*-methylated Trost ligand (**2Me-L3**) under the standard conditions. As shown in Fig. 4A, no reaction occurred with oxindole-derived VCP **1a** remained unconsumed, indicating the important role of hydrogen bond in catalytic efficiency. To further shed light on the stereoinduction mechanism, detailed DFT calculations were performed employing the ωB97XD/SMD/6-311+G** (SDD for Pd)// ωB97XD/6-31G* (lanl2dz for Pd) level of theory. As shown in Fig. 4B, four pre-reaction intermediates (**A–D**) were captured in different binding modes with the catalyst. Interestingly, the cyclopropane ring was still closed in **A** and **C**, while it was open in **B** and **D** because of the H-bonding interaction between the amide in the chiral ligand and the carbonyl group in the substrate, which stabilized the negative charge on the carbonyl oxygen after ring opening. Starting from these four intermediates, eight reaction pathways were fully explored, the details of which can be found in Section 7 of the Supplementary Information (SI). We focused on the four optimal reaction pathways leading to the four stereoisomers, as shown in Fig. 4B. All pathways involved two main steps: an ester-formation step (*O*-addition of the enol moiety to the ketene), followed by a ring-formation step (intramolecular allylic substitution of the newly formed enol moiety). For pathways starting from **A** and **C**, the first step (**TS1** and **TS2**) was a concerted step in which C–O bond formation was accompanied by cyclopropane ring opening, unlike the ester-formation step starting from **B** and **D** (**TS3** and **TS4**, respectively), in which the cyclopropane ring was already open. Consequently, the energies of **TS3** and **TS4** were significantly lower than those of **TS1** and **TS2**.

As shown in Fig. 4C, further NCI analysis revealed that the hydrogen bond between the amide of the chiral ligand (*50*) and the oxygen atom of the enol intermediate could still be found in **TS3**, but not in any other ester-formation transition states, including **TS4**. We suggested that such H-bonding interaction stabilizes **TS3** and further lowers the energy barrier from **B** to **K**. The π-π stacking interaction between the phenyl group in ligand and the indole group in the substrate located by NCI also provided some stabilization effect for **TS3**. Therefore, the overall energy barrier of the **B**-**K** pathway (**TS7** instead of **TS3**, 18.3 kcal/mol) was lower than that of **A**-**I** (**TS1**, 25.2 kcal/mol), **C**-**J** (**TS2**, 27.6 kcal/mol), and **D**-**L** (**TS4**, 20.0 kcal/mol). **K** was predicted to be the major product, in good agreement with the experimentally observed major product **(S_p, *S*)-3a**, which explained >90% ee and >19:1 dr values. We conclude that the well-positioned H-bond is a crucial source of Pd-catalyzed [7+2] cycloaddition stereoselectivity by stabilizing the ring-opening intermediates and favoring the transition state for the ester-formation step. Notably, we also investigated the ring size selectivity and found that the nine-membered ring product was significantly favored over the seven-membered ring product because of the relatively low steric repulsion in the former (see Section 7.2 in SI for more details). In conclusion, the results presented herein not only open a new avenue for the asymmetric synthesis of planar-chiral cycloalkenes, but also significantly expand the frontier of Pd-catalyzed higher-order cycloadditions.

Demonstrating the utility and generality of present strategy

The results reported herein represent an efficient and straightforward method for the modular synthesis of planar-chiral 9-membered cycloalkenes from readily available starting materials. To further demonstrate the utility of this methodology, a scale-up reaction between VCP **1a** and phenyl-substituted diazoacetate **4a** was performed, affording the desired product **5a** almost with the same efficiency and stereoselectivity. Following, several synthetic transformations were performed using product **5a**. First, strongly acidic condition was used to remove the Boc protecting group on the indole moiety, affording the desired N-H product **6a** in 84% yield without affecting the labile planar chirality of the cycloalkene (Fig. 5A, Eq. 1). Second, we demonstrated that planar-chiral cycloalkenes can serve as synthetically valuable handles to access other central-chiral functional groups (Fig. 5A, Eqs. 2-4). For example, the Diels–Alder reaction between cycloalkene **5a** and a tetrazine derivative (*47*) afforded the new chiral medium-sized heterocycle **6b** in 95% yield. Epoxidation and cyclopropanation reactions were performed according to previously reported procedures (*48*, *49*) to afford corresponding products **6c** and **6d** in 99% and 81% yields, respectively. The enantio- and diastereo-purities of these products were nearly retained during the conversion from planar chirality to central chirality, and the stereochemistry was established by analyzing the X-ray crystal structure of chiral product **6c**.

Furthermore, this cycloaddition strategy for planar-chiral cycloalkenes was successfully extended beyond oxindole-derived VCPs. Under similar catalytic conditions, the pyrrole-derived cyclic allylic ester **7** was suitable for the Pd-catalyzed [7+2] cycloaddition with a variety of diazo reagents **2** in the presence of a catalytic amount of $Rh_2(OAc)_4$. Enantioenriched pyrrole-fused cycloalkenes **8a-8d** can be afforded in 56-71% yields with up to 97% ee and >19:1 dr (Fig. 5B, Eq. 1). In addition, the *β*-naphthol-derived linear allylic ester **9** can be used for this higher-order cycloaddition with diazo reagents **4** by simply optimizing the reaction conditions. Naphthyl-fused cycloalkenes **10a-10c** were prepared in 50-74% yields with up to 92% ee and >19:1 dr (Fig. 5B, Eq. 2). These results demonstrate the generality of higher-order cycloaddition strategy for the modular synthesis of planar-chiral cycloalkenes.

References and Notes

1. R. López, C. Palomo, Planar chirality: a mine for catalysis and structure discovery. *Angew. Chem. Int. Ed.* **61**, e202113504 (2021). doi: 10.1002/anie.202113504
2. J. Li, D. Huang, Q. Fang, C. Zhao, Progress on synthesis of optically pure mechanical planar chiral rotaxanes and planar chiral macrocycle molecules. *Chin. Sci. Bull.* **677**, 2383–2392 (2022). doi: 10.1360/TB-2021-1324
3. G. C. Fu, Applications of planar-chiral heterocycles as ligands in asymmetric catalysis. *Acc. Chem. Res.* **39**, 853–860 (2006). doi: 10.1021/ar068115g
4. L.-X. Dai, X.-L. Hou, *Chiral Ferrocenes in Asymmetric Catalysis* (Wiley, 2010).
5. T. Muraoka, K. Kinbara, T. Aida, Mechanical twisting of a guest by a photoresponsive host. *Nature* **440**, 512–515 (2006). doi: 10.1038/nature04635
6. M. Patra, G. Gasser, The medicinal chemistry of ferrocene and its derivatives. *Nat. Rev. Chem.* **1**, 0066 (2017). doi: 10.1038/s41570-017-0066
7. E. M. Carreira, L. Kvaerno, *Classics in Stereoselective Synthesis* (Wiley, 2009).
8. B. Tan, *Axially Chiral Compounds: Asymmetric Synthesis and Applications* (Wiley, 2021).

9. K. Tanaka, H. Sagae, K. Toyoda, K. Noguchi, M. Hirano, Enantioselective synthesis of planar-chiral metacyclophanes through rhodium-catalyzed alkyne cyclotrimerization. *J. Am. Chem. Soc.* **129**, 1522–1523 (2007). doi: 10.1021/ja0679127

10. T. Shibata, T. Uchiyama, K. Endo, Enantioselective synthesis of chiral tripodal cage compounds by [2 + 2 + 2] cycloaddition of branched triynes. *Org. Lett.* **11**, 3906–3908 (2009). doi: 10.1021/ol9014893

11. K. Kanda, K. Endo, T. Shibata, Enantioselective synthesis of planar-chiral 1,*n*-dioxa[*n*]paracyclophanes via catalytic asymmetric *ortho*-lithiation. *Org. Lett.* **12**, 1980–1983 (2010). doi: 10.1021/ol100444u

12. T. Araki, K. Noguchi, K. Tanaka, Enantioselective synthesis of planar-chiral carba-paracyclophanes: rhodium-catalyzed [2+2+2] cycloaddition of cyclic diynes with terminal monoynes. *Angew. Chem. Int. Ed.* **52**, 5617–5621 (2013). doi: 10.1002/anie.201300696

13. K. Igawa, et al., Catalytic enantioselective synthesis of planar-chiral cyclic amides based on a Pd-catalyzed asymmetric allylic substitution reaction. *J. Am. Chem. Soc.* **137**, 7294–7297 (2015). doi: 10.1021/jacs.5b04340

14. M.-L. Delcourt, S. Felder, E. Benedetti, L. Micouin, Highly enantioselective desymmetrization of centrosymmetric *pseudo-para*-diformyl[2.2]paracyclophane via asymmetric transfer hydrogenation. *ACS Catal.* **8**, 6612–6616 (2018). doi: 10.1021/acscatal.8b01872

15. C.-X. Liu, Q. Gu, S.-L. You, Asymmetric C–H bond functionalization of ferrocenes: new opportunities and challenges. *Trends Chem.* **2**, 737–749 (2020). doi: 10.1016/j.trechm.2020.05.003

16. M. Ogasawara, Enantioselective preparation of planar-chiral transition metal complexes by asymmetric olefin-metathesis reactions in metal coordination spheres. *Chem. Rec*. **21**, 3509–3519 (2021). doi: 10.1002/tcr.202100102

17. L. Zhou, et al., Synthesis of planar chiral ferrocenes via enantioselective remote C–H activation. *Nat. Chem.* **15**, 815–823 (2023). doi: 10.1038/s41557-023-01176-3

18. Gagnon, C. et al., Biocatalytic synthesis of planar chiral macrocycles. *Science* **367**, 917–921 (2020). doi: 10.1126/science.aaz7381

19. T. Q. N. Nguyen, et al., Post-translational formation of strained cyclophanes in bacteria. *Nat. Chem.* **12**, 1042–1053 (2020). doi: 10.1038/s41557-020-0519-z

20. R. L. Reyes, T. Iwai, M. Sawamura, Construction of medium-sized rings by gold catalysis. *Chem. Rev.* **121**, 8926–8947 (2021). doi: 10.1021/acs.chemrev.0c00793

21. K. Tomooka, N. Komine, D. Fujiki, T. Nakai, S. Yanagitsuru, Planar chiral cyclic ether: asymmetric resolution and chirality transformation. *J. Am. Chem. Soc.* **127**, 12182–12183 (2005). doi: 10.1021/ja053347g

22. R. Maeda, et al., Planar-to-planar chirality transfer in the excited state. enantiodifferentiating photoisomerization of cyclooctenes sensitized by planar-chiral paracyclophane. *J. Am. Chem. Soc.* **133**, 10379–10381 (2011). doi: 10.1021/ ja203781f

23. Y. Okayama, et al., Enantioselective synthesis of macrocyclic heterobiaryl derivatives of molecular asymmetry by molybdenum-catalyzed asymmetric ring-closing metathesis. *Angew. Chem. Int. Ed.* **54**, 4927–4931 (2015). doi: 10.1002/anie.201500459

24. C. Steinborn, et al., Total syntheses of (+)-waixenicin A, (+)-9-deacetoxy-14,15-deepoxyxeniculin, and (−)-xeniafaraunol A. *J. Am. Chem. Soc.* **145**, 11811–11817 (2023). doi: 10.1021/jacs.3c03366

25. H. Tamamura, K. Hiramatsu, S. Ueda, et al., Stereoselective synthesis of [l-arg-l/d-3-(2-naphthyl)alanine]-type (*E*)-alkene dipeptide isosteres and its application to the synthesis and biological evaluation of pseudopeptide analogues of the CXCR4 antagonist FC131. *J. Med. Chem.* **48**, 380–391 (2005). doi: 10.1021/jm049429h

26. O. Pàmies, et al., Recent advances in enantioselective Pd-catalyzed allylic substitution: from design to applications. *Chem. Rev.* **121**, 4373–4505 (2021). doi: 10.1021/acs.chemrev.0c00736

27. M.-M. Zhang, B.-L. Qu, B. Shi, W.-J. Xiao, L.-Q. Lu, High-order dipolar annulations with metal-containing reactive dipoles. *Chem. Soc. Rev.* **51**, 4146–4174 (2022). doi: 10.1039/d1cs00897h

28. L.-C. Yang, et al., Construction of nine-membered heterocycles through palladium-catalyzed formal [5+4] cycloaddition. *Angew. Chem. Int. Ed.* **56**, 2927–2931 (2017). doi: 10.1002/anie.201611474

29. A. Khan, et al., Palladium-catalyzed decarboxylative cycloaddition of vinylethylene carbonates with formaldehyde: enantioselective construction of tertiary vinylglycols. *Angew. Chem. Int. Ed.* **53**, 6439–6442 (2014). doi: 10.1002/anie.201403754

30. A. Khan, L. Yang, J. Xu, L. Y. Jin, Y. J. Zhang, Palladium-catalyzed asymmetric decarboxylative cycloaddition of vinylethylene carbonates with michael acceptors: construction of vicinal quaternary stereocenters. *Angew. Chem. Int. Ed.* **53**, 11257–11260 (2014). doi: 10.1002/anie.201407013

31. S. Singha, T. Patra, C. G. Daniliuc, F. Glorius, Highly enantioselective [5 + 2] annulations through cooperative n-heterocyclic carbene (nhc) organocatalysis and palladium catalysis. *J. Am. Chem. Soc.* **140**, 3551–3554 (2018). doi: 10.1021/jacs.8b00868

32. Y.-N. Wang, et al., Pd-catalyzed enantioselective [6+4] cycloaddition of vinyl oxetanes with azadienes to access ten-membered heterocycles. *Angew. Chem. Int. Ed.* **57**, 1596–1600 (2018). doi: 10.1002/anie.201711648

33. Y. Wei, et al., Enantioselective trapping of Pd-containing 1,5-dipoles by photogenerated ketenes: access to 7-membered lactones bearing chiral quaternary stereocenters. *J. Am. Chem. Soc.* **141**, 133–137 (2019). doi: 10.1021/jacs.8b12095

34. H. Uno, N. Punna, E. Tokunaga, M. Shiro, N. Shibata, Synthesis of both enantiomers of nine-membered CF_3-substituted heterocycles using a single chiral ligand: palladium-catalyzed decarboxylative ring expansion with kinetic resolution. *Angew. Chem. Int. Ed.* **59**, 8187–8194 (2020). doi: 10.1002/anie.201915021

35. Q. Zhang, et al., Palladium-catalyzed asymmetric [8+2] dipolar cycloadditions of vinyl carbamates and photogenerated ketenes. *Angew. Chem. Int. Ed.* **59**, 14096–14100 (2020). doi: 10.1002/anie.202005313

36. G. Yang, Y. Ke, Y. Zhao, Stereoselective access to polyfunctionalized nine-membered heterocycles by sequential gold and palladium catalysis. *Angew. Chem. Int. Ed.* **60**, 12775–12780 (2021). doi: 10.1002/anie.202102061

37. B. Shi, et al., Synthesis of chiral endocyclic allenes by palladium-catalyzed asymmetric annulation followed by Cope rearrangement. *Angew. Chem. Int. Ed.* **61**, e202117215 (2022). doi: 10.1002/anie.202117215

38. X. Jiang, et al., Construction of axial chirality via asymmetric radical trapping by cobalt under visible light. *Nat. Catal.* **5**, 788–797 (2022). doi: 10.1038/s41929-022-00831-1

39. B.-C. Wang, et al., De novo construction of chiral aminoindolines by Cu-catalyzed asymmetric cyclization and subsequent discovery of an unexpected sulfonyl migration. *J. Am. Chem. Soc.* **144**, 19932–19941 (2022). doi: 10.1021/jacs.2c08090

40. Y. Xiao, et al., Taming chiral quaternary stereocenters via remote h-bonding stereoinduction in palladium-catalyzed (3+2) cycloadditions. *Angew. Chem. Int. Ed.* **62**, e202212444 (2023). doi: 10.1002/anie.202212444

41. R. Jiang, L. Ding, C. Zheng, S.-L. You, Iridium-catalyzed Z-retentive asymmetric allylic substitution reactions. *Science* **371**, 308–386 (2021). doi: 10.1126/science.abd6095

42. M. Meazza, R. Rios, Synergistic catalysis: enantioselective ring expansion of vinyl cyclopropanes combining four catalytic cycles for the synthesis of highly substituted spirocyclopentanes bearing up to four stereocenters. *Chem. Eur. J.* **22**, 9923–9928 (2016). doi: 10.1002/chem.201601893

43. M. D. Mandler, P. M. Truong, P. Y. Zavalij, M. P. Doyle, Catalytic conversion of diazocarbonyl compounds to imines: applications to the synthesis of tetrahydropyrimidines and β-lactams. *Org. Lett.* **16**, 740–743 (2014). doi: 10.1021/ol403427s

44. M.-M. Li, et al., Utilizing vinylcyclopropane reactivity: palladium-catalyzed asymmetric [5+2] dipolar cycloadditions. *Angew. Chem. Int. Ed.* **59**, 17429–17434 (2020). doi: 10.1002/anie.202006366

45. X.-P. Zeng, Z.-Y. Cao, Y.-H. Wang, F. Zhou, J. Zhou, Catalytic enantioselective desymmetrization reactions to all-carbon quaternary stereocenters. *Chem. Rev.* **116**, 7330–7396 (2016). doi: 10.1021/acs.chemrev.6b00094

46. L. Süsse, B. M. Stoltz, Enantioselective formation of quaternary centers by allylic alkylation with first-row transition-metal catalysts. *Chem. Rev.* **121**, 4084–4099 (2021). doi: 10.1021/acs.chemrev.0c01115

47. Fang, Y. et al., Photochemical syntheses, transformations, and bioorthogonal chemistry of trans-cycloheptene and sila trans-cycloheptene Ag(I) complexes. *Chem Sci.* **9**, 1953-1963 (2018). doi: 10.1039/c7sc04773h

48. K. Tomooka, M. Suzuki, M. Shimada, R. Ni, K. Uehara, Stereoselective multimodal transformations of planar chiral 9-membered diallylic amides. *Org. Lett.* **13**, 4926-4929 (2011). doi: 10.1021/ol202009x

49. T. Ito, et al., Synthesis of functionalized medium-sized *trans*-cycloalkenes by 4π electrocyclic ring opening/alkylation sequence. *Angew. Chem. Int. Ed.* **58**, 11836-11840 (2019). doi: 10.1002/anie.201906665

50. C. P. Butts, et al., Structure-based rationale for selectivity in the asymmetric allylic alkylation of cycloalkenyl esters employing the Trost 'Standard Ligand' (TSL): isolation, analysis and alkylation of the monomeric form of the cationic η^3-cyclohexenyl complex [(η^3-*c*-C_6H_9)Pd(TSL)]$^+$. *J. Am. Chem. Soc.* **131**, 9945–9957 (2009). doi: 10.1021/ja8099757

Acknowledgments: This paper is dedicated to the 120th anniversary of Central China Normal University (CCNU) and the 100th birth anniversary of the Honorable Mr. Lixin Dai. We thank Prof. Fang-Fang Pan (CCNU) for X-ray crystallographic analysis assistance. We gratefully acknowledge Prof. Wen-Bo Liu in Wuhan University and Prof. Zhihan Zhang in CCNU for helpful discussions.

Funding:

National Natural Science Foundation of China (22271113)

National Natural Science Foundation of China (21971056)

National Natural Science Foundation of China (91956201)

National Natural Science Foundation of China (21820102003)

Founding from Central China Normal University

Founding from Wuhan Institute of Photochemistry and Technology

Author contributions:

Conceptualization: LQL

Methodology: ZXZ, YLTF, YHL, BJZ, YQX, YJL

Funding acquisition: WJX, LQL

Project administration: WJX, LQL

Supervision: YR, YT, LQL

Writing – original draft: ZXZ, LR, YHL

Writing – review & editing: YR, YT, WJX, LQL

Competing interests: Authors declare that they have no competing interests.

Data and materials availability: Crystallographic data for the structures reported in this paper have been deposited at the Cambridge Crystallographic Data Centre under deposition numbers (CCDC) as CCDC 2283029 (the epoxide of **3a''**), CCDC 2291246 (**3a1''**), 2284114 (**5p**), 2283030 (**6c**) and 2344652 (**10a**). Copies of the data can be obtained free of charge via https://www.ccdc.cam.ac.uk/structures/. All other characterization data are in the supplementary materials. All data are available in the main text or the supplementary materials.

Supplementary Materials

Materials and Methods

Figs. S1-S6

Tables S1 to S4

NMR and HPLC Data

References (*51–58*)

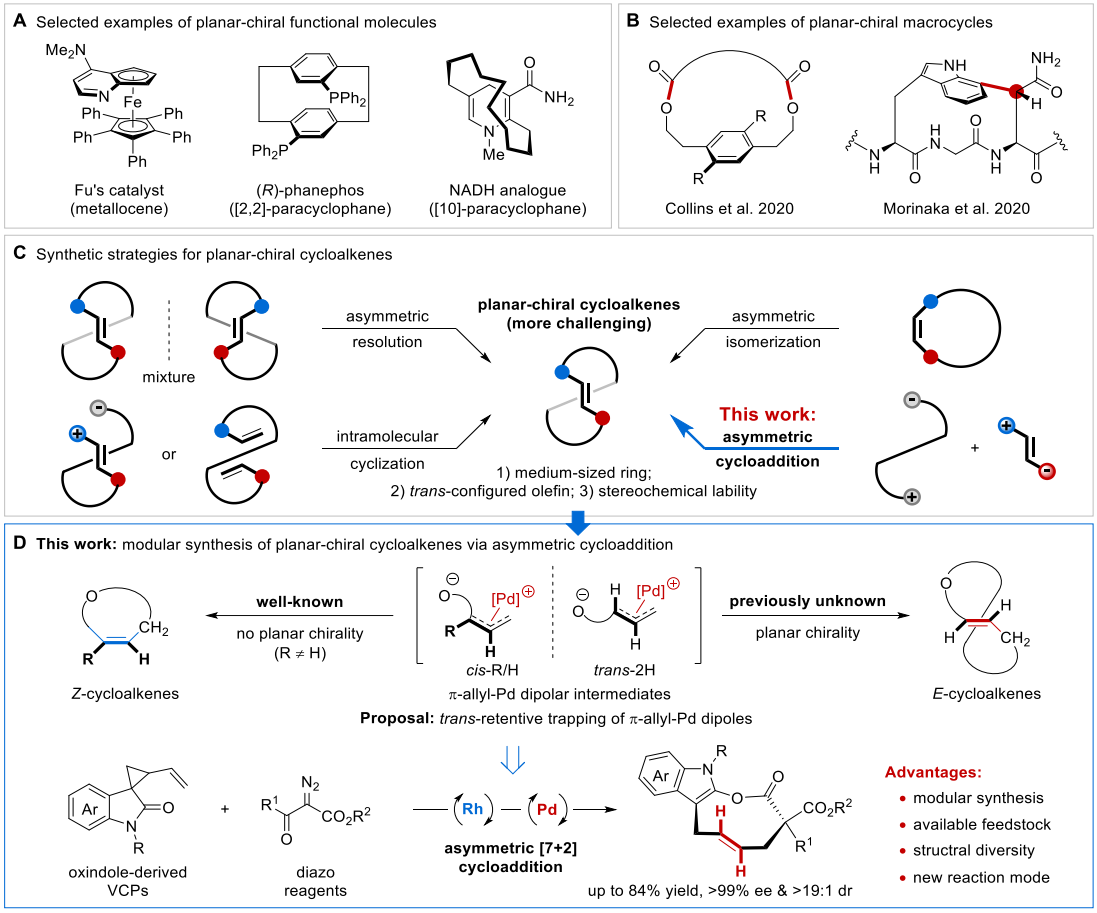

Fig. 1. Strategies to access planar-chiral cycloalkenes. (**A**) Selected examples of planar-chiral functional molecules. (**B**) Selected examples of planar-chiral macrocycles. (**C**) Synthetic strategies for planar-chiral cycloalkenes. (**D**) This work: modular synthesis of planar-chiral cycloalkenes via asymmetric cycloaddition.

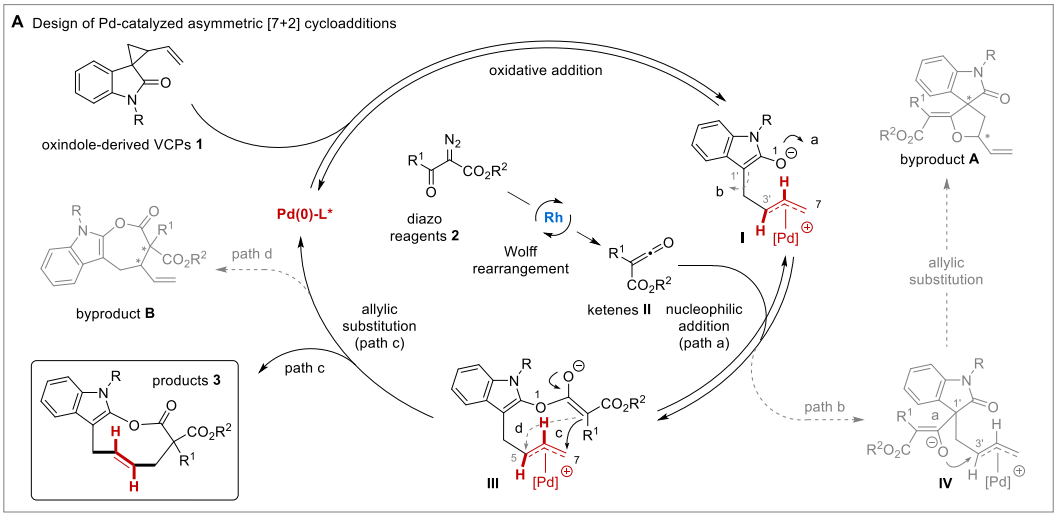

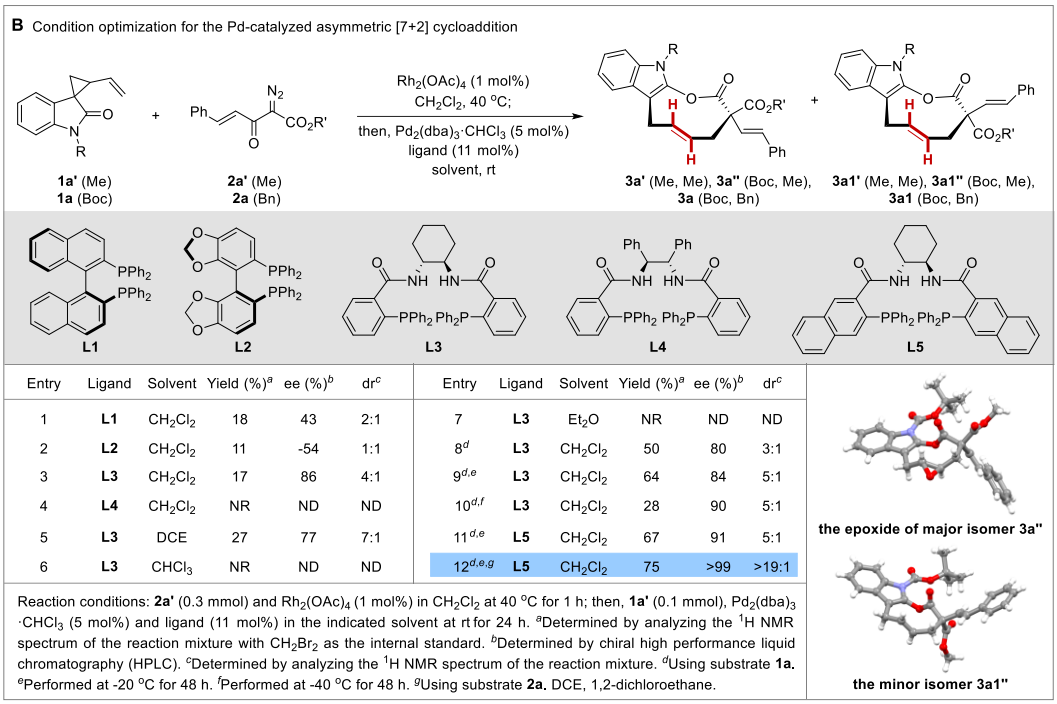

Entry	Ligand	Solvent	Yield (%)[a]	ee (%)[b]	dr[c]
1	**L1**	CH_2Cl_2	18	43	2:1
2	**L2**	CH_2Cl_2	11	-54	1:1
3	**L3**	CH_2Cl_2	17	86	4:1
4	**L4**	CH_2Cl_2	NR	ND	ND
5	**L3**	DCE	27	77	7:1
6	**L3**	$CHCl_3$	NR	ND	ND
7	**L3**	Et_2O	NR	ND	ND
8[d]	**L3**	CH_2Cl_2	50	80	3:1
9[d,e]	**L3**	CH_2Cl_2	64	84	5:1
10[d,f]	**L3**	CH_2Cl_2	28	90	5:1
11[d,e]	**L5**	CH_2Cl_2	67	91	5:1
12[d,e,g]	**L5**	CH_2Cl_2	75	>99	>19:1

Reaction conditions: **2a'** (0.3 mmol) and $Rh_2(OAc)_4$ (1 mol%) in CH_2Cl_2 at 40 °C for 1 h; then, **1a'** (0.1 mmol), $Pd_2(dba)_3$·$CHCl_3$ (5 mol%) and ligand (11 mol%) in the indicated solvent at rt for 24 h. [a]Determined by analyzing the ^1H NMR spectrum of the reaction mixture with CH_2Br_2 as the internal standard. [b]Determined by chiral high performance liquid chromatography (HPLC). [c]Determined by analyzing the ^1H NMR spectrum of the reaction mixture. [d]Using substrate **1a**. [e]Performed at -20 °C for 48 h. [f]Performed at -40 °C for 48 h. [g]Using substrate **2a**. DCE, 1,2-dichloroethane.

Fig. 2. Reaction design and condition optimization. (**A**) Reaction blueprint of Pd-catalyzed asymmetric [7+2] cycloadditions. (**B**) Condition optimization for the Pd-catalyzed asymmetric [7+2] cycloaddition. Bn, benzyl; Boc, *tert*-butyloxycarbonyl; ee, enantiomeric excess; Me, methyl; ND, not determined; NR, no reaction.

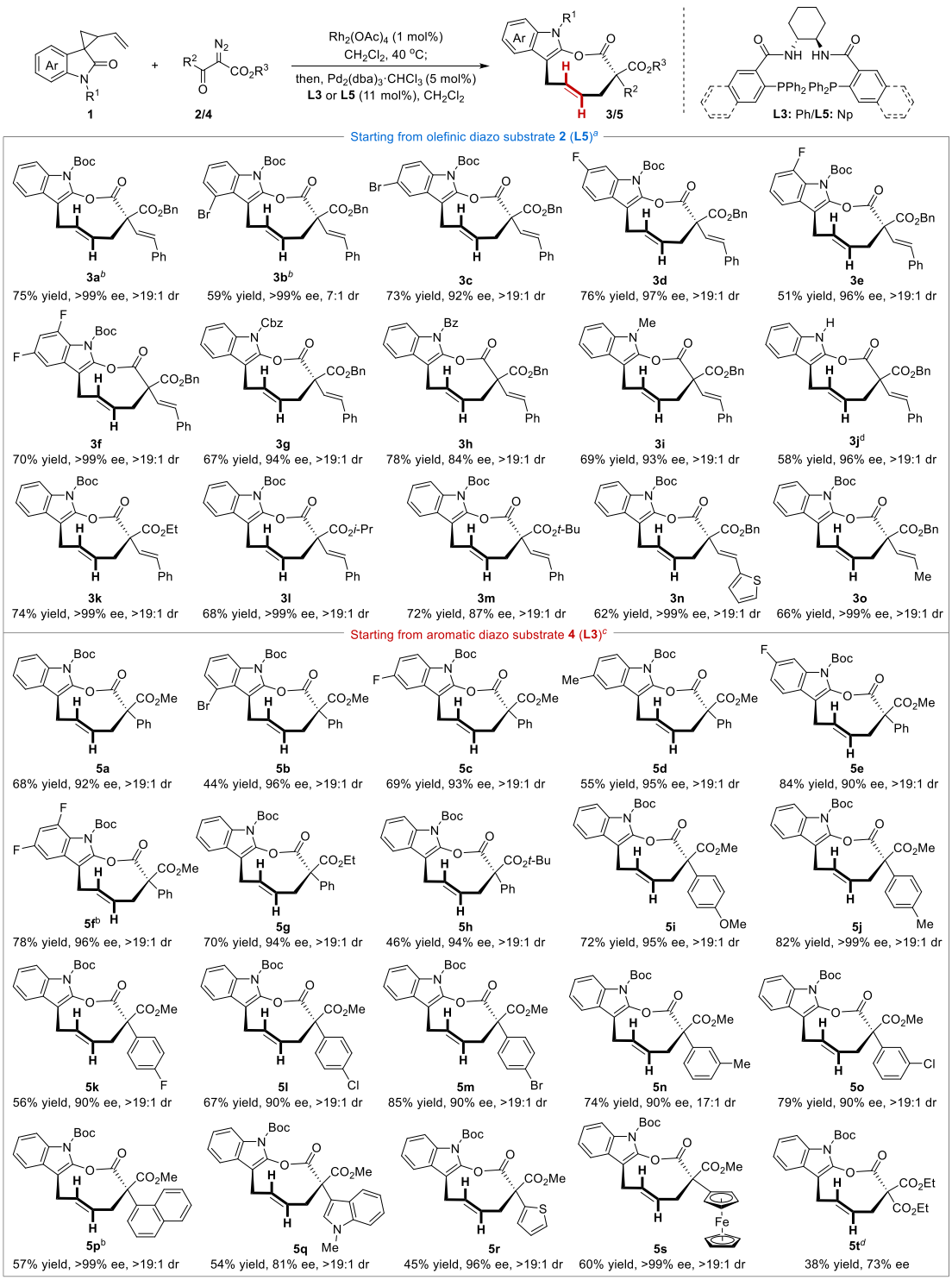

[a]Reaction conditions: the same with entry 12 in Fig. 1 except reaction temprature and time (0 °C, 24 h). [b]The ee value was determined after epoxidation. [c]Reaction conditions: the same with entry 12 in Fig. 1 except ligand, reaction temprature and time (**L3**, 0 °C, 24 h). [d]Ketene was generated by the photochemical method (see the details in SI).

Fig. 3. Scope of asymmetric [7+2] cycloadditions. Bz, benzoyl; Cbz, carbobenzoxy; Et, ethyl; *i*-Pr, *iso*-propyl.

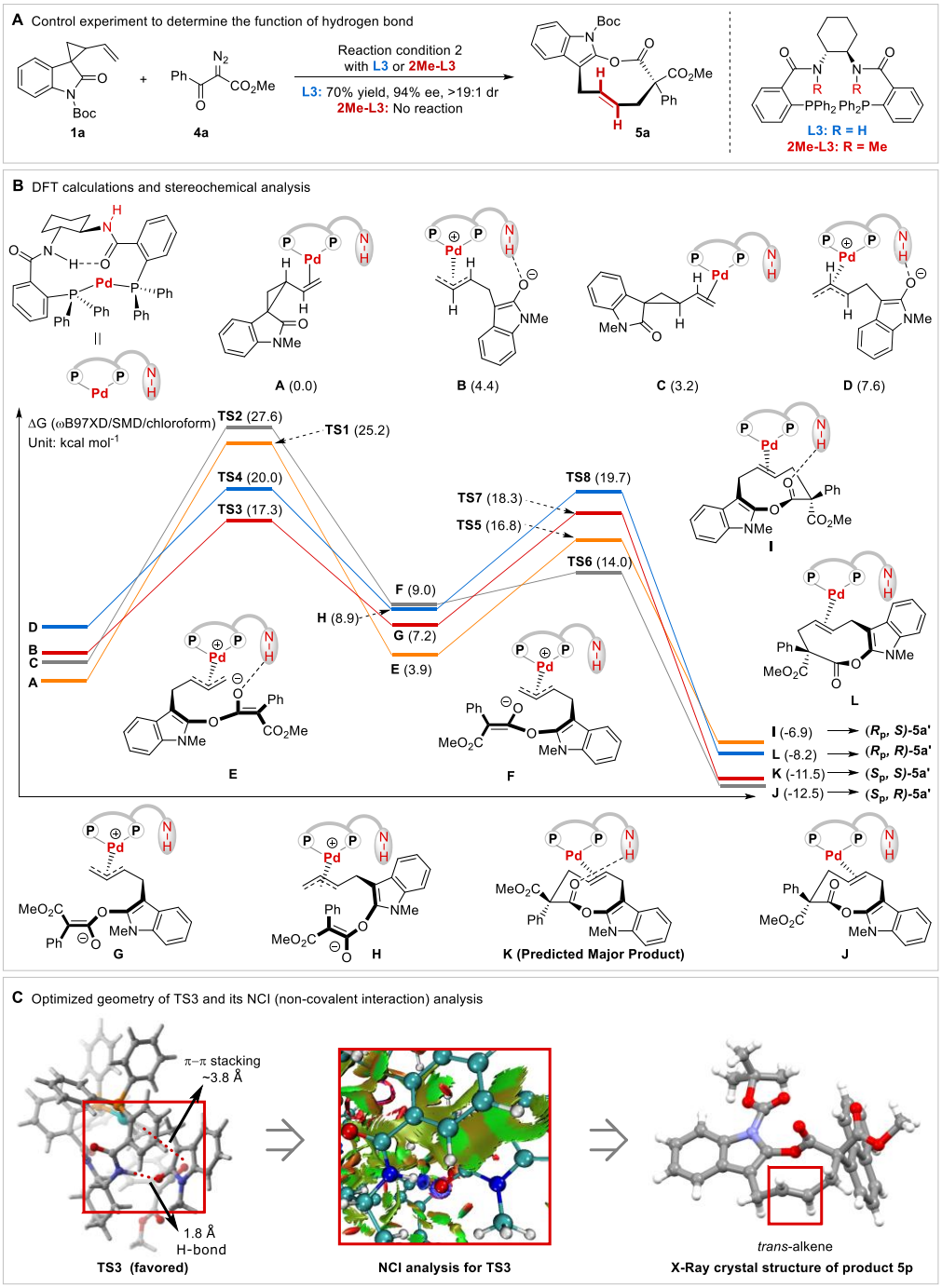

Fig. 4. Mechanism investigation of the asymmetric cycloaddition. (**A**) Control experiment to determine the function of hydrogen bond. (**B**) DFT calculations and stereochemical analysis. Data in parentheses is the calculated relative energy in reference to compound **A**. (**C**) Optimized geometry of **TS3** and its NCI (non-covalent interaction) analysis. These analysis reveals the vital H-bond between the chiral ligand amide and the substrate carbonyl group as well as π-π stacking in **TS3**. In NCI plot, the blue region indicates attraction, green region represents for Van der Walls interaction, and red region denotes repulsive interaction.

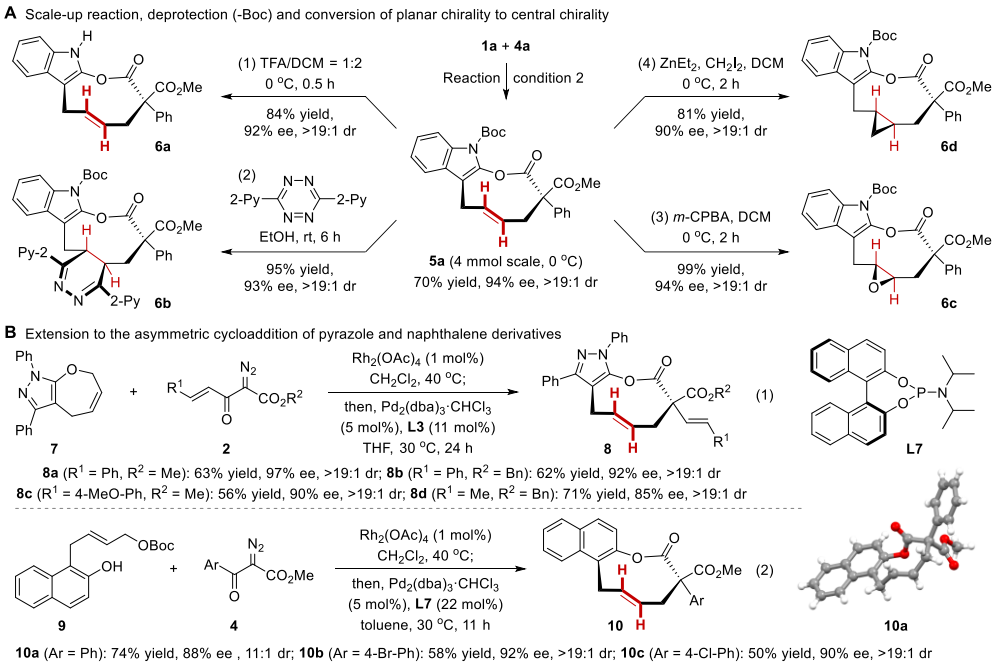

Fig. 5. Demonstration of the utility and generality of synthetic strategy. (A) Scale-up reaction, deprotection (-Boc) and conversion of planar chirality to central chirality. **(B)** Extension to the asymmetric [7+2] cycloaddition of pyrazole and naphthalene derivatives.